Available online at www.sciencedirect.com
ScienceDirect
Journal of Sound and Vibration 305 (2007) 543–551
JOURNAL OF SOUND AND VIBRATION
www.elsevier.com/locate/jsvi

Short Communication

Free vibration analysis of non-cylindrical helical springs by the pseudospectral method

Jinhee Lee*

Department of Mechano-Informatics, Hongik University, Chochiwon, Yeonki-kun, Choongnam 339-701, Republic of Korea

Received 12 January 2007; received in revised form 2 April 2007; accepted 8 April 2007
Available online 5 July 2007

Abstract

The pseudospectral method is applied to the free vibration analysis of non-cylindrical helical springs. The entire domain is considered as a single element and the displacements and the rotations are approximated by the sums of Chebyshev polynomials. The internal forces and moments are substituted to give six equations of motion, which are collocated to yield the system of algebraic equations. The boundary condition is considered as the constraints, and the set of equations is condensed so that the number of degrees of freedom of the problem matches the number of the expansion coefficients. Numerical examples are provided for clamped–clamped, free–free, clamped–free and hinged–hinged boundary conditions.

1. Introduction

Previous investigations on the free vibration of non-cylindrical helical springs [1–6] were based on the multi-element methods such as the transfer matrix method. The set of equations was expressed as

$$\frac{\mathrm{d}}{\mathrm{d}\theta}\{X(\theta)\} = [Z]\{X(\theta)\} \tag{1}$$

with the state vector

$$\{X(\theta)\} = \{U_t U_n U_b \Omega_t \Omega_n \Omega_b F_t F_n F_b M_t M_n M_b\}^{\mathrm{T}}, \tag{2}$$

where the differential matrix $[Z]$ was a function of $R(\theta)$. U, Ω, F and M represent the displacements, the rotations, the internal forces and the internal moments, respectively. Subscripts t, n and b stand for the tangential direction, the normal direction and the binormal direction. Because the horizontal radius $R(\theta)$ is not constant for non-cylindrical helical springs they had to employ relatively large number of elements to compute the natural frequencies. Busool and Eisenberger [7] set six equations of motion, where $\mathrm{d}R(\theta)/\mathrm{d}\theta$ as well as $R(\theta)$ was included, and computed the natural frequencies with a smaller number of elements.

Recently, Lee [8] applied the pseudospectral method to the free vibration analysis of cylindrical helical springs. In the pseudospectral method, the entire domain is considered as a single element and the governing

*Tel.: +82 16 9321 2589; fax: +82 41 862 2664.
E-mail address: jinhlee@wow.hongik.ac.kr.

0022-460X/$ - see front matter
doi:10.1016/j.jsv.2007.04.017

equations are collocated at a number of collocation points inside the element. Since each spectral coefficient is determined by all the collocation point values the pseudospectral method can be made as spatially accurate as desired through exponential rate of convergence with grid refinement. Moreover, neither numerical differentiation nor numerical integration process is associated with the present method. The differentiations of basis functions can be performed analytically, which enhances the accuracy of the solution of the pseudospectral method.

2. Formulations for non-cylindrical helical springs

Figs. 1 and 2 describe typical non-cylindrical helical springs and the schematic geometry of a helical spring. $R(\theta)$ is given for barrel and hyperboloidal types from

$$R(\theta) = R_1 + (R_2 - R_1)\left(1 - \frac{2\theta}{\Theta}\right)^2 \tag{3}$$

and for conical type from

$$R(\theta) = R_1 + (R_2 - R_1)\frac{\theta}{\Theta}, \tag{4}$$

where $(0 \leqslant \theta \leqslant \Theta = 2\pi n_c)$ and n_c is the number of turns of the helix.

Yildirim [2] derived the equations of motion for the free vibration of a helical spring as

$$F_t' - CF_n = -\omega^2 \frac{\rho AR}{C} U_t, \quad F_n' + CF_t - SF_b = -\omega^2 \frac{\rho AR}{C} U_n, \tag{5a,b}$$

$$F_b' + SF_n = -\omega^2 \frac{\rho AR}{C} U_b, \quad M_t' - CM_n = -\omega^2 \frac{\rho JR}{C} \Omega_t, \tag{5c,d}$$

$$M_n' - \frac{R}{C} F_b + CM_t - SM_b = -\omega^2 \frac{\rho I_n R}{C} \Omega_n, \quad M_b' + \frac{R}{C} F_n + SM_n = -\omega^2 \frac{\rho I_b R}{C} \Omega_b \tag{5e,f}$$

at natural frequency ω in rad/s, where the notation $'$ stands for the differentiation with respect to θ. C and S represent $\cos\alpha$ and $\sin\alpha$, where α is the pitch angle of the helix. A, I_n, I_b and J are the cross-sectional area, the

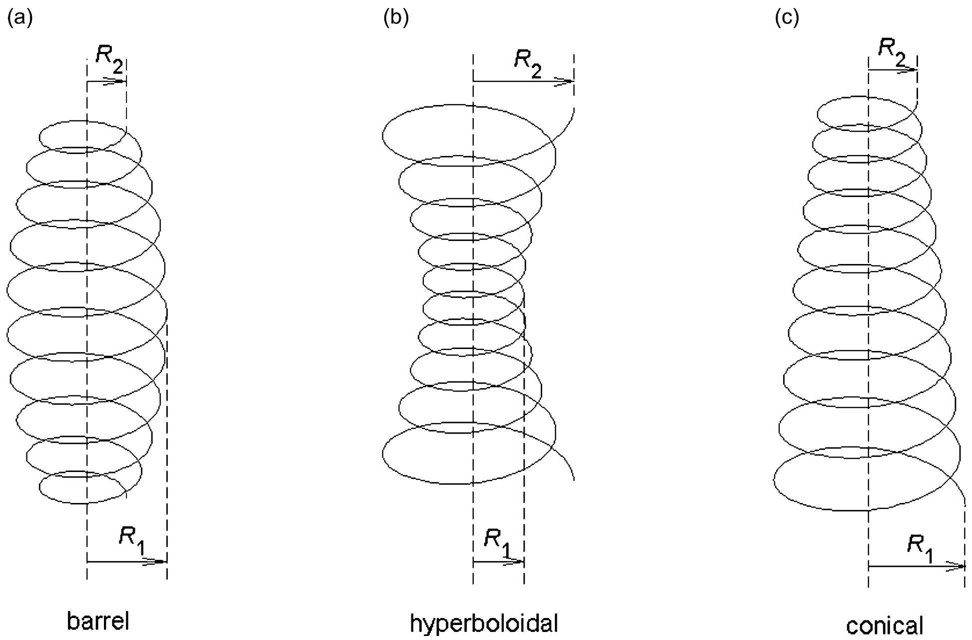

Fig. 1. Non-cylindrical helical springs.

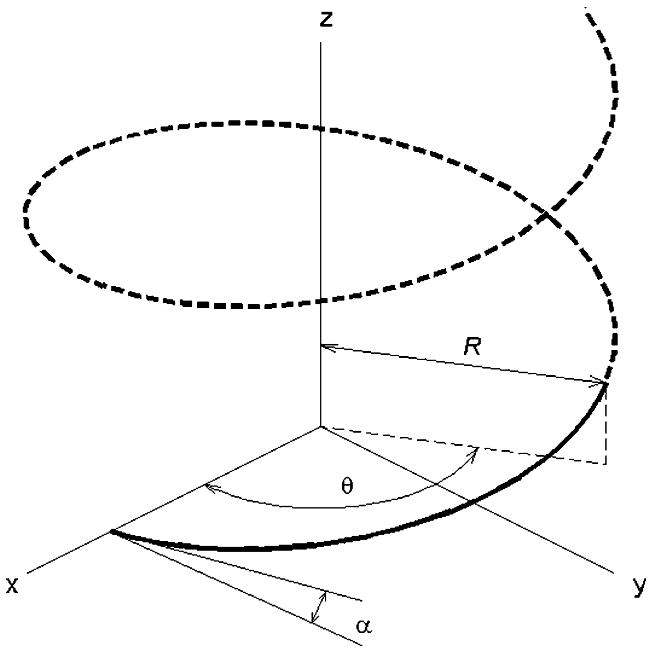

Fig. 2. Schematic geometry of a helical spring.

second moments of area with respect to the normal axis and to the binormal axis, and the torsional moment of inertia of the cross-section.

When the range of the independent variable is given by ($0\leqslant\theta\leqslant\Theta$), it is convenient to use the normalized variable

$$\xi = \frac{2\theta - \Theta}{\Theta} \in [-1, 1]. \tag{6}$$

The displacements and the rotations are expressed as sums of Chebyshev polynomials as follows:

$$\begin{aligned} U_t(\xi) &= \sum_{k=1}^{K+2} a_k T_{k-1}(\xi), \quad U_n(\xi) = \sum_{k=1}^{K+2} b_k T_{k-1}(\xi), \quad U_b(\xi) = \sum_{k=1}^{K+2} c_k T_{k-1}(\xi), \\ \Omega_t(\xi) &= \sum_{k=1}^{K+2} d_k T_{k-1}(\xi), \quad \Omega_n(\xi) = \sum_{k=1}^{K+2} e_k T_{k-1}(\xi), \quad \Omega_b(\xi) = \sum_{k=1}^{K+2} f_k T_{k-1}(\xi), \end{aligned} \tag{7}$$

where a_k, b_k, c_k, d_k, e_k and f_k are the expansion coefficients. K is the number of collocation points. $T_k(\xi)$ is the Chebyshev polynomial of the first kind defined as

$$T_k(\xi) = T_k(\cos\phi) = \cos k\phi \quad (-1\leqslant\xi\leqslant 1), \tag{8}$$

where $\phi = \cos^{-1}\xi$. Its derivatives with respect to ξ are

$$\begin{cases} \mathrm{d}T_k(\xi)/\mathrm{d}\xi = k \sin k\phi / \sin\phi, \\ \mathrm{d}^2 T_k(\xi)/\mathrm{d}\xi^2 = -k^2 \cos k\phi / \sin^2\phi + k \cos\phi \cos k\phi / \sin^3\phi \quad (-1<\xi<1) \end{cases} \tag{9}$$

and

$$\mathrm{d}^n T_k/\mathrm{d}\xi^n\big|_{\xi=\pm 1} = (\pm 1)^{k+n} \prod_{p=0}^{n-1} (k^2 - p^2)/(2p+1) \tag{10}$$

at $\xi = \pm 1$.

F_t, F_n, F_b, M_t, M_n and M_b for a helical spring of constant cross-section are extracted from the remaining six equations of Yildirim [2] and expansions (7) are applied to result in

$$F_t(\xi) = \frac{EA}{R}\left(U_t' - C^2 U_n\right) = \frac{EA}{R}\sum_{k=1}^{K+2}\left\{\frac{2a_k}{\Theta}T^*_{k-1}(\xi) - b_k C^2 T_{k-1}(\xi)\right\}, \tag{11a}$$

$$\begin{aligned} F_n(\xi) &= \frac{GA}{\beta}\left(\frac{U_n' + C^2 U_t - CSU_b}{R} - \Omega_b\right) \\ &= \frac{GA}{\beta}\sum_{k=1}^{K+2}\left\{\frac{2b_k}{R\Theta}T^*_{k-1}(\xi) + \left(\frac{a_k C^2 - c_k CS}{R} - f_k\right)T_{k-1}(\xi)\right\}, \end{aligned} \tag{11b}$$

$$\begin{aligned} F_b(\xi) &= \frac{GA}{\beta}\left(\frac{U_b'}{R} + \frac{CS}{R}U_n + \Omega_n\right) \\ &= \frac{GA}{\beta}\sum_{k=1}^{K+2}\left\{\frac{2c_k}{R\Theta}T^*_{k-1}(\xi) + \left(\frac{b_k CS}{R} + e_k\right)T_{k-1}(\xi)\right\}, \end{aligned} \tag{11c}$$

$$M_t(\xi) = \frac{GJ}{R}(\Omega_t' - C^2\Omega_n) = \frac{GJ}{R}\sum_{k=1}^{K+2}\left\{\frac{2d_k}{\Theta}T^*_{k-1}(\xi) - e_k C^2 T_{k-1}(\xi)\right\}, \tag{11d}$$

$$M_n(\xi) = \frac{EI_n}{R}(\Omega_n' + C^2\Omega_t - CS\Omega_b) = \frac{EI_n}{R}\sum_{k=1}^{K+2}\left\{\frac{2e_k}{\Theta}T^*_{k-1}(\xi) + (d_k C^2 - f_k CS)T_{k-1}(\xi)\right\}, \tag{11e}$$

$$M_b(\xi) = \frac{EI_b}{R}(\Omega'_b + CS\Omega_n) = \frac{EI_b}{R}\sum_{k=1}^{K+2}\left\{\frac{2f_k}{\Theta}T^*_{k-1}(\xi) + e_k CST_{k-1}(\xi)\right\}. \tag{11f}$$

The notation * stands for the differentiation with respect to ξ. E, G and β are Young's modulus, the shear modulus and the Timoshenko coefficient, respectively.

Eqs. (7) and (11a)–(11f) are substituted into Eqs. (5a)–(5f), and are collocated at the Gauss–Lobatto collocation points

$$\xi_i = -\cos\frac{\pi(2i-1)}{2K} \quad (i = 1, 2, \ldots, K) \tag{12}$$

to yield the collocated governing equations as given below:

$$\begin{aligned} &\sum_{k=1}^{K+2} a_k\left\{\frac{4EAC}{R_i\Theta^2}T^{**}_{k-1}(\xi_i) - \frac{2EAR_i'C}{R_i^2\Theta}T^*_{k-1}(\xi_i) - \frac{GAC^3}{\beta R_i}T_{k-1}(\xi_i)\right\} \\ &+ \sum_{k=1}^{K+2} b_k\left\{-\left(EA + \frac{GA}{\beta}\right)\frac{2C^2}{R_i\Theta}T^*_{k-1}(\xi_i) + \frac{EAR_i'C^2}{R_i^2}T_{k-1}(\xi_i)\right\} \\ &+ \sum_{k=1}^{K+2} c_k\frac{GAC^2S}{\beta}T_{k-1}(\xi_i) + \sum_{k=1}^{K+2} f_k\frac{GAC}{\beta}T_{k-1}(\xi_i) \\ &= -\omega^2\frac{\rho A}{C}\sum_{k=1}^{K+2} a_k R_i T_{k-1}(\xi_i), \end{aligned} \tag{13a}$$

$$
\begin{aligned}
&\sum_{k=1}^{K+2} a_k\left\{\left(EA+\frac{GA}{\beta}\right)\frac{2C^2}{R_i\Theta}T^*_{k-1}(\xi_i)-\frac{GAR'_iC^2}{\beta R_i^2}T_{k-1}(\xi_i)\right\}\\
&\quad+\sum_{k=1}^{K+2} b_k\left\{\frac{4GAC}{\beta R_i\Theta^2}T^{**}_{k-1}(\xi_i)-\frac{2GAR'_iC}{\beta R_i^2\Theta}T^*_{k-1}(\xi_i)-\left(EAC^2+\frac{GAS^2}{\beta}\right)\frac{C}{R_i}T_{k-1}(\xi_i)\right\}\\
&\quad+\sum_{k=1}^{K+2} c_k\left\{-\frac{4GACS}{\beta R_i\Theta}T^*_{k-1}(\xi_i)+\frac{GAR'_iCS}{\beta R_i^2}T_{k-1}(\xi_i)\right\}\\
&\quad-\sum_{k=1}^{K+2} e_k\frac{GAS}{\beta}T_{k-1}(\xi_i)-\sum_{k=1}^{K+2} f_k\frac{2GA}{\beta\Theta}T^*_{k-1}(\xi_i)\\
&\quad=-\omega^2\frac{\rho A}{C}\sum_{k=1}^{K+2} b_kR_iT_{k-1}(\xi_i),
\end{aligned}
\tag{13b}
$$

$$
\begin{aligned}
&\sum_{k=1}^{K+2} a_k\frac{GAC^2S}{\beta R_i}T_{k-1}(\xi_i)+\sum_{k=1}^{K+2} b_k\left\{\frac{4GACS}{\beta R_i\Theta}T^*_{k-1}(\xi_i)-\frac{GAR'_iCS}{\beta R_i^2}T_{k-1}(\xi_i)\right\}\\
&\quad+\sum_{k=1}^{K+2} c_k\left\{\frac{4GAC}{\beta R_i\Theta^2}T^{**}_{k-1}(\xi_i)-\frac{2GAR'_iC}{\beta R_i^2\Theta}T^*_{k-1}(\xi_i)-\frac{GACS^2}{\beta R_i}T_{k-1}(\xi_i)\right\}\\
&\quad+\sum_{k=1}^{K+2} e_k\frac{2GA}{\beta\Theta}T^*_{k-1}(\xi_i)-\sum_{k=1}^{K+2} f_k\frac{GAS}{\beta}T_{k-1}(\xi_i)\\
&\quad=-\omega^2\frac{\rho A}{C}\sum_{k=1}^{K+2} c_kR_iT_{k-1}(\xi_i),
\end{aligned}
\tag{13c}
$$

$$
\begin{aligned}
&\sum_{k=1}^{K+2} d_k\left\{\frac{4GJC}{R_i\Theta^2}T^{**}_{k-1}(\xi_i)-\frac{2GJR'_iC}{R_i^2\Theta}T^*_{k-1}(\xi_i)-\frac{EI_nC^3}{R_i}T_{k-1}(\xi_i)\right\}\\
&\quad+\sum_{k=1}^{K+2} e_k\left\{-(GJ+EI_n)\frac{2C^2}{R_i\Theta}T^*_{k-1}(\xi_i)+\frac{GJR'_iC^2}{R_i^2}T_{k-1}(\xi_i)\right\}\\
&\quad+\sum_{k=1}^{K+2} f_k\frac{EI_nC^2S}{R_i}T_{k-1}(\xi_i)\\
&\quad=-\omega^2\frac{\rho J}{C}\sum_{k=1}^{K+2} d_kR_iT_{k-1}(\xi_i),
\end{aligned}
\tag{13d}
$$

$$
\begin{aligned}
&-\sum_{k=1}^{K+2} b_k\frac{GAS}{\beta}T_{k-1}(\xi_i)-\sum_{k=1}^{K+2} c_k\frac{2GA}{\beta\Theta}T^*_{k-1}(\xi_i)\\
&\quad+\sum_{k=1}^{K+2} d_k\left\{(EI_n+GJ)\frac{2C^2}{R_i\Theta}T^*_{k-1}(\xi_i)-\frac{EI_nR'_iC^2}{R_i^2}T_{k-1}(\xi_i)\right\}\\
&\quad+\sum_{k=1}^{K+2} e_k\left\{\frac{4EI_nC}{R_i\Theta^2}T^{**}_{k-1}(\xi_i)-\frac{2EI_nR'_iC}{R_i^2\Theta}T^*_{k-1}(\xi_i)\right.\\
&\quad\left.-\left(\frac{GAR_i}{\beta C}+\frac{GJC^3}{R_i}+\frac{EI_bCS^2}{R_i}\right)T_{k-1}(\xi_i)\right\}
\end{aligned}
$$

$$+\sum_{k=1}^{K+2} f_k\left\{-(EI_n+EI_b)\frac{2CS}{R_i\Theta}T^*_{k-1}(\xi_i)+\frac{EI_nR'_iCS}{R_i^2}T_{k-1}(\xi_i)\right\}$$
$$=-\omega^2\frac{\rho I_n}{C}\sum_{k=1}^{K+2} e_kR_iT_{k-1}(\xi_i), \tag{13e}$$

$$\sum_{k=1}^{K+2} a_k\frac{GAC}{\beta}T_{k-1}(\xi_i)+\sum_{k=1}^{K+2} b_k\frac{2GA}{\beta\Theta}T^*_{k-1}(\xi_i)-\sum_{k=1}^{K+2} c_k\frac{GAS}{\beta}T_{k-1}(\xi_i)$$
$$+\sum_{k=1}^{K+2} d_k\frac{EI_nC^2S}{R_i}T_{k-1}(\xi_i)+\sum_{k=1}^{K+2} e_k\left\{(EI_n+EI_b)\frac{2CS}{R_i\Theta}T^*_{k-1}(\xi_i)-\frac{EI_bR'_iCS}{R_i^2}T_{k-1}(\xi_i)\right\}$$
$$+\sum_{k=1}^{K+2} f_k\left\{\frac{4EI_bC}{R_i\Theta^2}T^{**}_{k-1}(\xi_i)-\frac{2EI_bR'_iC}{R_i^2\Theta}T^*_{k-1}(\xi_i)-\left(\frac{GAR_i}{\beta C}+\frac{EI_nCS^2}{R_i}\right)T_{k-1}(\xi_i)\right\}$$
$$=-\omega^2\frac{\rho I_b}{C}\sum_{k=1}^{K+2} f_kR_iT_{k-1}(\xi_i) \quad (i=1,\ldots,K). \tag{13f}$$

R_i and R'_i represent $R(\xi_i)$ and $\mathrm{d}R(\xi_i)/\mathrm{d}\theta$, respectively. Eqs. (13a)–(13f) can be rearranged in the matrix form

$$[B]\{\delta\}+[D]\{\gamma\}=\omega^2([P]\{\delta\}+[Q]\{\gamma\}), \tag{14}$$

where the vectors in Eq. (14) are defined by

$$\begin{aligned}\{\delta\}&=\{a_1a_2\cdots a_K\ \ b_1b_2\cdots b_K\ \ c_1c_2\cdots c_K\ \ d_1d_2\cdots d_K\ \ e_1e_2\cdots e_K\ \ f_1f_2\cdots f_K\}^{\mathrm{T}},\\ \{\gamma\}&=\{a_{K+1}\ \ a_{K+2}\ \ b_{K+1}\ \ b_{K+2}\ \ c_{K+1}\ \ c_{K+2}\ \ d_{K+1}\ \ d_{K+2}\ \ e_{K+1}\ \ e_{K+2}\ \ f_{K+1}\ \ f_{K+2}\}^{\mathrm{T}}.\end{aligned} \tag{15}$$

The total number of equations in Eqs. (13a)–(13f) is $6K$ whereas the total number of unknown expansion coefficients is $6(K+2)$. The remaining 12 equations are obtained from the boundary conditions. Typical boundary conditions are represented by

$$\text{clamped}:\quad U_t=0,\quad U_n=0,\quad U_b=0,\quad \Omega_t=0,\quad \Omega_n=0,\quad \Omega_b=0, \tag{16a}$$

$$\text{hinged}:\quad U_t=0,\quad U_n=0,\quad U_b=0,\quad M_t=0,\quad M_n=0,\quad M_b=0, \tag{16b}$$

$$\text{free}:F_t=0,\quad F_n=0,\quad F_b=0,\quad M_t=0,\quad M_n=0,\quad M_b=0. \tag{16c}$$

For example when the series expansions of Eqs. (7) and (11a)–(11f) are substituted into the clamped–clamped boundary condition at $\xi=\pm1$, the boundary condition set in the spectral form is expressed as

$$\begin{aligned}&\sum_{k=1}^{K+2} a_kT_{k-1}(-1)=0,\quad \sum_{k=1}^{K+2} b_kT_{k-1}(-1)=0,\quad \sum_{k=1}^{K+2} c_kT_{k-1}(-1)=0,\\ &\sum_{k=1}^{K+2} d_kT_{k-1}(-1)=0,\quad \sum_{k=1}^{K+2} e_kT_{k-1}(-1)=0,\quad \sum_{k=1}^{K+2} f_kT_{k-1}(-1)=0,\\ &\sum_{k=1}^{K+2} a_kT_{k-1}(1)=0,\quad \sum_{k=1}^{K+2} b_kT_{k-1}(1)=0,\quad \sum_{k=1}^{K+2} c_kT_{k-1}(1)=0,\\ &\sum_{k=1}^{K+2} d_kT_{k-1}(1)=0,\quad \sum_{k=1}^{K+2} e_kT_{k-1}(1)=0,\quad \sum_{k=1}^{K+2} f_kT_{k-1}(1)=0,\end{aligned} \tag{17}$$

which acts as the constraints of Eqs. (13a)–(13f). The boundary condition set in the spectral form can be rearranged in the matrix form

$$[V]\{\delta\}+[W]\{\gamma\}=\{0\} \tag{18}$$

and Eq. (14) can be reformulated as

$$([B]-[D][W]^{-1}[V])\{\delta\}=\omega^2([P]-[Q][W]^{-1}[V])\{\delta\}. \quad (19)$$

The solution of Eq. (19) yields the estimate for the natural frequencies and the expansion coefficients. The formulation is straightforward and easy for writing the code.

Table 1
Convergence test of the natural frequencies in Hz (hyperboloidal helix, $R_2/R_1=2.4$, $R_1=13$ mm, $\alpha=4.8^\circ$, wire radius $r=1.3$ mm, $A=\pi r^2$, $I_n=I_b=\pi r^4/4$, $J=\pi r^4/2$, $n_c=6.5$, $v=0.3$, $E=210$ GPa, $\rho=7850\,\text{kg/m}^3$, $\beta=1.1$, clamped–clamped boundary condition)

	ω_1	ω_2	ω_3	ω_4	ω_5	ω_6
Present study						
$K=20$	76.483	125.327	180.509	194.008	235.289	264.569
$K=30$	75.783	97.014	97.175	133.488	160.471	184.298
$K=40$	75.762	96.311	103.086	133.212	160.702	184.316
$K=50$	75.762	96.311	103.086	133.212	160.702	184.316
Busool–Eisenberger [7] (7 elements)	75.762	96.312	103.087	133.213	160.702	184.316

Table 2
Natural frequencies in Hz of a hyperboloidal-type helical spring ($R_1=13$ mm, $r=1.3$ mm, $A=\pi r^2$, $I_n=I_b=\pi r^4/4$, $J=\pi r^4/2$, $n_c=6.5$, $\alpha=4.8^\circ$, $\beta=1.1$, $E=210$ GPa, Poisson's ratio $v=0.3$, $\rho=7850\,\text{kg/m}^3$, clamped–clamped boundary condition, $K=50$)

R_2/R_1	ω_1	ω_2	ω_3	ω_4	ω_5
1.2					
Present study	178.93	208.80	227.83	238.45	360.07
Yildirim [2]	178.94	208.80	227.85	238.46	360.07
1.6					
Present study	130.29	159.62	170.74	193.59	271.12
Yildirim [2]	130.29	159.63	170.76	193.60	271.12
2.0					
Present study	97.85	122.69	131.07	160.03	205.82
Yildirim [2]	97.85	122.69	131.08	160.03	205.82
2.4					
Present study	75.76	96.31	103.09	133.21	160.70
Yildirim [2]	75.76	96.31	103.10	133.22	160.70

Table 3
Natural frequencies in Hz of a barrel-type helical spring ($R_1=25$ mm, $r=1$ mm, $A=\pi r^2$, $I_n=I_b=\pi r^4/4$, $J=\pi r^4/2$, $n_c=6.5$, $\alpha=4.8^\circ$, $\beta=1.1$, $E=210$ GPa, $v=0.3$, $\rho=7850\,\text{kg/m}^3$, clamped–clamped boundary condition, $K=50$)

R_2/R_1	ω_1	ω_2	ω_3	ω_4	ω_5
0.2					
Present study	71.86	81.19	99.94	99.95	143.88
Yildirim [2]	71.86	81.19	99.95	99.96	143.88
0.4					
Present study	65.53	71.52	86.93	87.00	129.60
Yildirim [2]	65.53	71.52	86.94	87.01	129.60
0.6					
Present study	59.62	61.79	75.07	75.08	114.01
Yildirim [2]	59.62	61.78	75.08	75.09	114.01
0.8					
Present study	52.11	54.57	64.46	64.76	99.15
Yildirim [2]	52.11	54.57	64.46	64.77	99.15

3. Numerical examples

The algorithm developed in the preceding section was realized by a program written in Matlab, and a preliminary run was carried out to check the convergence of the natural frequencies of a hyperboloidal helical spring for $R_2/R_1 = 2.4$ for clamped–clamped boundary condition and the results are given in Table 1. The number of collocation points, which had impact on the accuracy of the solution ranged from $K = 20$ to 50. Table 1 shows that the solution was converged for the six lowest natural frequencies to five significant figures for $K < 40$. The converged frequencies are in excellent agreement with the results of Busool–Eisenberger [7].

The natural frequencies were computed for hyperboloidal-type, barrel-type and conical-type helical springs and the results are given in Tables 2–4. It is found that the computational results in Tables 2–4 are in good agreement with those of Yildirim [2,6]. The largest discrepancy between them is found in the case of conical spring when R_2/R_1 is close to unity, of which relative error is less than 0.05%.

Any set of boundary condition can be merged into the collocated governing equations systematically by the procedure explained in Eqs. (17)–(19). The natural frequencies computed by the pseudospectral method for clamped–clamped, free–free, clamped–free and hinged–hinged boundary conditions are given in Table 5.

Table 4
Natural frequencies in Hz of a conical-type helical spring ($R_1 = 5\,\text{mm}$, $r = 0.5\,\text{mm}$, $A = \pi r^2$, $I_n = I_b = \pi r^4/4$, $J = \pi r^4/2$, $n_c = 7.6$, $\alpha = 8.5744^\circ$, $\beta = 1.1$, $E = 206.1\,\text{GPa}$, $v = 0.3$, $\rho = 7900\,\text{kg/m}^3$, clamped–clamped boundary condition, $K = 50$)

R_2/R_1	ω_1	ω_2	ω_3	ω_4	ω_5	ω_6
0.9						
Present study	435.73	438.56	512.74	581.45	955.83	970.39
Yildirim [6]	435.65	438.43	512.62	581.32	955.73	969.98
0.8						
Present study	484.58	487.63	571.14	644.10	1060.6	1076.8
Yildirim [6]	484.49	487.47	571.00	643.96	1060.5	1076.3
0.7						
Present study	541.32	544.58	639.89	714.23	1179.7	1197.9
Yildirim [6]	541.23	544.39	639.72	714.08	1179.6	1197.3
0.6						
Present study	607.47	610.98	720.96	792.42	1314.5	1335.8
Yildirim [6]	607.37	610.74	720.77	792.24	1314.4	1335.2
0.5						
Present study	684.76	688.76	816.06	879.38	1465.5	1492.7
Yildirim [6]	684.64	688.48	815.82	879.17	1465.4	1491.9

Table 5
Natural frequencies in Hz of a hyperboloidal-barrel-type helical springs ($R_1 = 13\,\text{mm}$, $r = 1.3\,\text{mm}$, $A = \pi r^2$, $I_n = I_b = \pi r^4/4$, $J = \pi r^4/2$, $n_c = 6.5$, $\alpha = 4.8^\circ$, $\beta = 1.1$, $E = 210\,\text{GPa}$, $v = 0.3$, $\rho = 7850\,\text{kg/m}^3$, $K = 50$)

R_2/R_1	Boundary condition	ω_1	ω_2	ω_3	ω_4	ω_5	ω_6
0.5 (barrel)	Clamped–clamped	300.40	319.00	387.25	387.53	583.96	613.70
	Hinged–hinged	189.75	197.38	337.50	363.26	467.76	499.64
	Free–free	264.34	362.37	375.48	375.88	542.17	634.94
	Clamped–free	89.91	90.09	144.86	165.41	346.97	348.59
2 (hyperboloidal)	Hinged–hinged	43.97	46.94	122.46	122.56	159.96	174.84
	Free–free	109.29	115.35	125.23	145.94	191.98	231.99
	Clamped–free	35.17	35.35	55.38	63.05	112.15	123.60

4. Conclusions

The pseudospectral method is applied to the free vibration analysis of non-cylindrical helical springs and numerical examples are provided for clamped–clamped, free–free, clamped–free and hinged–hinged boundary conditions. The displacements and the rotations are approximated by the series expansions of Chebyshev polynomials. The equations of motion include $\mathrm{d}R(\theta)/\mathrm{d}\theta$ as well as $R(\theta)$, and the entire domain is considered as a single element. The equations of motion are collocated to yield the collocated governing equations, from which the natural frequencies are computed. To handle the boundary condition the number of collocation points is chosen to be less than the number of the expansion terms. The boundary condition is considered as the constraints of the governing equations, and the set of algebraic equations is condensed so that the number of degrees of freedom of the problem matches the total number of the expansion coefficients. The results of present study show good agreement with those of the published literature.

Acknowledgment

This work was supported by 2007 Hongik University Research Fund.

References

[1] K. Nagaya, S. Takeda, Y. Nakata, Free vibration of coil springs of arbitrary shape, *International Journal for Numerical Methods in Engineering* 23 (1986) 1081–1099.
[2] V. Yildirim, Free vibration of non-cylindrical coil springs by combined use of the transfer matrix and the complementary functions methods, *Communications in Numerical Methods in Engineering* 13 (1997) 487–494.
[3] V. Yildirim, N. İnce, Natural frequencies of helical springs of arbitrary shape, *Journal of Sound and Vibration* 204 (1997) 311–329.
[4] V. Yildirim, A parametric study on the free vibration of noncylindrical helical springs, *Journal of Applied Mechanics* 65 (1998) 157–163.
[5] V. Yildirim, Free vibration characteristics of composite barrel and hyperboloidal coil springs, *Mechanics of Composite Materials and Structures* 8 (3) (2001) 205–217.
[6] V. Yildirim, A parametric study on the natural frequencies of unidirectional composite conical springs, *Communications in Numerical Methods in Engineering* 20 (2004) 207–227.
[7] W. Busool, M. Eisenberger, Free vibration of helicoidal beams of arbitrary shape and variable cross section, *Journal of Vibration and Acoustics* 124 (2002) 397–409.
[8] J. Lee, Free vibration analysis of cylindrical helical springs by the pseudospectral method, *Journal of Sound and Vibration* 302 (2007) 185–196.